Self-Immobilizing Fusion Enzymes for Compartmentalized Biocatalysis

Theo Peschke, Marc Skoupi, Teresa Burgahn, Sabrina Gallus, Ishtiaq Ahmed, Kersten S. Rabe, and Christof M. Niemeyer*

Institute for Biological Interfaces (IBG 1), Karlsruhe Institute of Technology (KIT), Hermann von Helmholtz Platz 1, 76344 Eggenstein Leopoldshafen, Germany

ABSTRACT: The establishment of microfluidic enzyme cascades is a topical field of research and development, which is currently hampered by the lack of methodologies for mild and efficient immobilization of isolated enzymes. We here describe the use of self immobilizing fusion enzymes for the modular configuration of microfluidic packed bed reactors. Specifically, three different enzymes, the (*R*) selective alcohol dehydrogenase LbADH, the (*S*) selective methylglyoxal reductase Gre2p and the NADP(H) regeneration enzyme glucose 1 dehydrogenase GDH, were genetically fused with streptavidin binding peptide, Spy and Halo based tags, to enable their specific and directional immobilization on magnetic microbeads coated with complementary receptors. The enzyme modified beads were loaded in four channel microfluidic chips to create compartments that have the capability for either (*R*) or (*S*) selective reduction of the prochiral C_S symmetrical substrate 5 nitrononane 2,8 dione (NDK). Analysis of the isomeric hydroxyketone and diol products by chiral HPLC was used to quantitatively characterize the performance of reactors configured with different amounts of the enzymes. Long operating times of up to 14 days indicated stable enzyme immobilization and the general robustness of the reactor. Even more important, by fine tuning of compartment size and loading, the overall product distribution could be controlled to selectively produce a single *meso* diol with nearly quantitative conversion (>95%) and excellent stereoselectivity (d.r. > 99:1) in a continuous flow process. We believe that our concept will be expandable to a variety of other biocatalytic or chemo enzymatic cascade reactions.

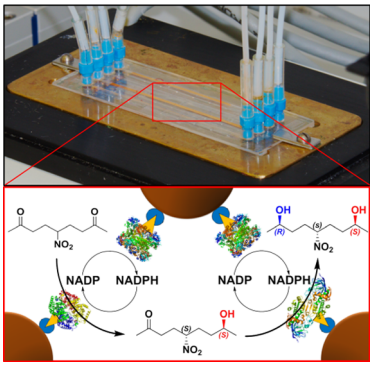

KEYWORDS: *enzyme cascade, biocatalysis, immobilization techniques, stereoselective reactions, modular microreactor*

INTRODUCTION

Biocatalytic transformations are considered as a key domain of industrial biotechnology for the conversion and efficient use of renewable biomass as an alternative to petrochemical synthesis for sustainable production processes and energy supply in the future.[1] Enzymes are the work horses in these developments because of their substrate scope and selectivity, which can be tailored to the process requirements by protein engineering and even de novo design.[2] A rich source of innovation in biocatalysis is currently drawn from biomimetic approaches for the compartmentalization and cascading of multiple enzymatic transformations.[3−7] One important approach to implement enzyme cascades into future biocatalytic processes takes adavantage of compartmentalized microfluidic reactors. Microfluidics offer a high level of control over temperature profiles and diffusion based mixing,[8,9] which is mandatory for the rational improvement of biocatalytic processes. However, a major challenge in the establishment of microfluidic enzyme cascades concerns the immobilization of isolated enzymes.[10] In most cases, purified enzymes are immobilized through nonspecific physisorption on charged carrier particles. However, this approach can lead to a strong decrease or even total loss of enzymatic activity.[9,10]

A more delicate and less harmful immobilization strategy relies on enzymes that are chemically tagged with affinity ligands, such as biotin[11,12] or DNA oligonucleotides.[13] However, since this strategy requires additional efforts for chemical modification and purification, genetically encoded immobilization tags are advantageous and they may even allow the direct immobilization from crude cell extracts. Indeed, hexahistidine (His) tagged enzymes have been exploited for cascade reactions carried out in flow systems[14−17] or on magnetic microbeads.[18,19] Since His tag immobilization is associated with a relatively low affinity ($K_d \sim 3\ \mu M$)[20] and specifity,[21] as well as potentially adverse effects on the activity of enzymes containing divalent metal ions,[22] there is a clear demand for generally applicable, mild and efficient techniques that allow for the immobilization of enzymes for fluidic processes.[3,23]

Toward this goal, we here describe the exploitation of high affinity tagging systems, which, to the best of our knowledge, have not yet been employed for enzymatic flow processes and microfluidic biocatalytic cascades. Self immobilizing fusion

Scheme 1. Sequential Enzymatic Reduction of the Prochiral C_s Symmetrical 5 Nitrononane 2,8 dione (NDK 1) Enables the Stereoselective Synthesis of the Stereoisomeric Hydroxyketones 2 and Diols 3: (A) Overview of All Possible Stereoisomers; (B) Three Enzyme, Two Step Reaction for the Reduction of NDK 1 to the *meso* Compound 3c

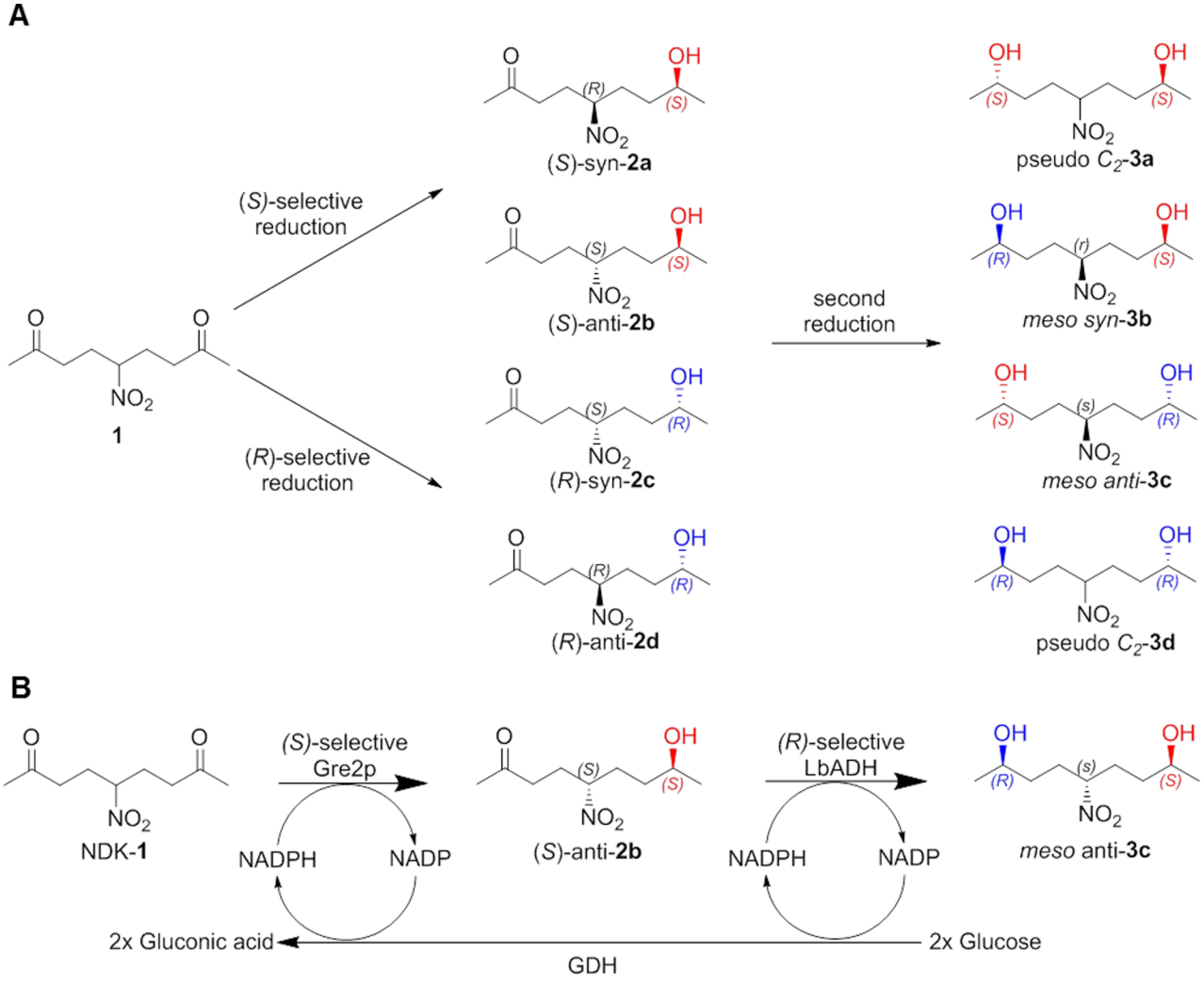

enzymes bearing such tags offer advantages since they immobilize enzymes under mild conditions while preserving activity and stereoselectivity. Furthermore, they would also save costs due to avoidance of cross linkers and simplification of immobilization processes, such as immobilization directly from crude cell extracts without any prior costly purification steps.

As a proof of concept, we chose the 39 amino acid streptavidin binding peptide (SBP) tag[24] that binds with high affinity ($K_d \sim 2{,}5$ nM) to the protein streptavidin (STV) and is often applied for chromatographic purification of recombinant proteins.[25] We demonstrate that these tag systems can be efficiently used for immobilization of several different stereo selective ketoreductase (KREDs) and cofactor regeneration enzymes to enable the facile fabrication of modular microfluidic packed bed reactors, which can be configured to produce distinctive stereoisomeric products that are not accessible by simple one pot syntheses. We also show that the SpyTag/SpyCatcher system[26] and a variant of the Halo tag system[27] can be used as orthogonal alternatives for the SBP/STV system to generate self immobilizing biocatalysts, which can be processed even from unpurified cell lysates.

RESULTS AND DISCUSSION

To explore and validate the utility of the SBP/STV system for microfluidic biocatalysis, we chose two stereoselective KREDs, the (*R*) selective alcohol dehydrogenase LbADH (EC 1.1.1.2) from *Lactobacillus brevis* ATCC 14869 (Taxonomy ID: 649758) and the (*S*) selective methylglyoxal reductase Gre2p (EC 1.1.1.283) from *Saccharomyces cerevisiae* YJM193 (Taxon omy ID: 1294304). As the substrate, we used the prochiral C_S symmetrical 5 nitrononane 2,8 dione (NDK) **1** (Scheme 1), which can be reduced, depending on the KRED selectivity, either on one or on both of the two carbonyl functions to create the hydroxyketones **2** or diols **3**, respectively (Scheme 1).[28] Since all stereoisomeric products can be readily analyzed by chiral HPLC, the enantiogroup differentiating reduction of the prochiral NDK **1** is ideally suited to evaluate and quantitatively analyze the biocatalytic activity of a given KRED system. To cope with the high demand for the structurally complex and expensive KRED cofactor, nicotina mide adenine dinucleotide phosphate (NADPH), we used the in situ NADP(H) regeneration enzyme (NRE) glucose 1 dehydrogenase GDH (EC 1.1.1.47) from *Bacillus subtilis* subsp. natto (Taxonomy ID: 86029). In comparison to other NRE systems, such as formiat/lactat decarboxylases, GDH does not

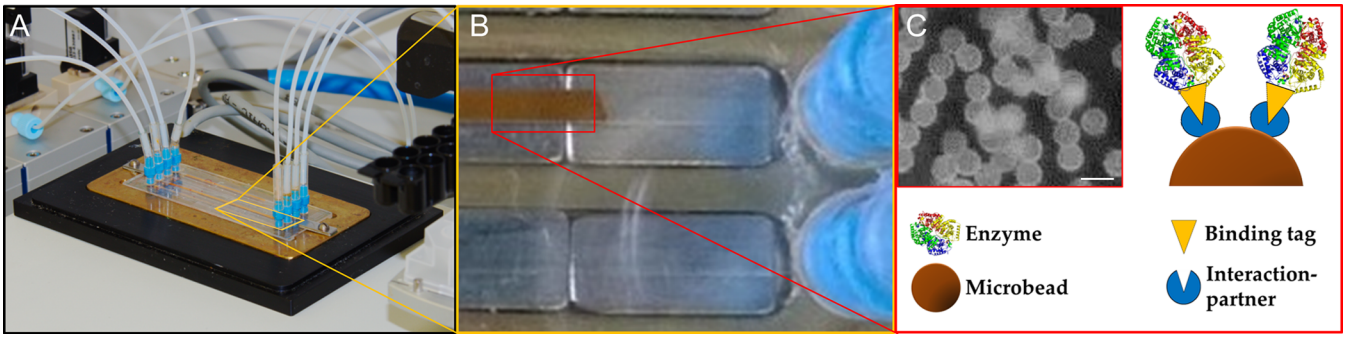

Figure 1. Compartmentalized microfluidic packed bed reactor loaded with enzyme functionalized magnetic particles. (A) The four channel PMMA chip is mounted in a temperature controlled chipholder which serves as chip to world interface. The four individual channel compartments can be connected by bridging tubes. (B) Image of two channel compartments with underlying rectangular Nd magnets that retain the enzyme functionalized superparamagnetic microbeads. (C) Schematic illustration and microscopy image of the microbeads that are functionalized with orthogonal interaction partners, which specifically bind to the corresponding tag, genetically fused to the enzyme of interest (scale bar = 3 μm).

Table 1. (A) Specific Enzyme Loading and (B) Activities of Free and Immobilized Enzymes on STV Coated Microbeads

A	MW	Homomeric subunits	Specific enzyme loading[a]	
	[$g_{protein}$ $mol_{subunit}^{-1}$]		[$\mu g_{protein}$ mg_{MB}^{-1}]	[$pmol_{subunit}$ mg_{MB}^{-1}]
GDH-SBP@MB-STV	36598	4	9.6 ± 0.6	262 ± 16
LbADH-SBP@MB-STV	32338		7.4 ± 0.3	229 ± 9
Gre2p-SBP@MB-STV	46640	1	11.8 ± 0.5	253 ± 11

B	MW	Homomeric subunits	Specific activty [b]		
	[$g_{protein}$ $mol_{subunit}^{-1}$]		[$nmol_{substrate}$ min^{-1} mg_{MB}^{-1}]	[$\mu mol_{substrate}$ min^{-1} $mg_{protein}^{-1}$]	[$\mu mol_{substrate}$ min^{-1} $\mu mol_{subunit}^{-1}$]
GDH-SBP	36598	4	-	0.9 ± 0.1	33 ± 4
GDH-SBP@MB-STV			8.0 ± 1.2	0.8 ± 0.2	30± 6
LbADH-SBP	32338		-	13.2 ± 0.3	427 ± 10
LbADH-SBP@MB-STV			85.4 ± 0.3	11.5 ± 0.5	373 ± 16
Gre2p-SBP	46640	1	-	2.2 ± 0.1	103 ± 5
Gre2p-SBP@MB-STV			24.2 ± 0.7	2.0 ± 0.1	96 ± 7

[a]Specific enzyme loading analyzed by comparative grayscale analysis. Specific enzyme loading data is normalized to protein subunits because Gre2p is a monomer,[32] while LbADH[29] and GDH[33] are homotetramers. Data represent the mean of triplicate analyzes ± 1 SD. [b]Specific activities of immobilized and free LbADH SBP, Gre2p SBP, and GDH SBP using NDK **1** and glucose as substrates. Data represent the mean of at least triplicate analyzes ± 1 SD (standard deviation). SD was calculated by error propagation of the data obtained from specific activity of bead immobilized enzymes and the specific enzyme loading.

produce CO_2 gas bubbles, which are detrimental for micro fluidic processes.

To study the performance of self immobilizing fusion enzymes in a compartmentalized microfluidic packed bed reactor (Figure 1), we initially focused on SBP tagged enzymes. To this end, SBP tagged LbADH, Gre2p and GDH were overexpressed in *E. coli* and purified to homogeneity using STV affinity chromatography (Figure S1). To investigate the reaction kinetics and stereoselectivity of the novel KRED SBPs, the purified enzymes were used for the reduction of NDK **1** substrate, and the hydroxyketone **2** and diol **3** products were analyzed by chiral HPLC. The (*R*) selective LbADH SBP produced (*R*) syn/anti hydroxyketones **2c/d** (e.r. >99:1; d.r. ~ 60:40). A fraction of these products is further reduced to the pseudo C_2 diol **3d** when glucose with an excess of GDH was used for cofactor recycling (Figure S3A). Since the LbADH can also act as its own NRE by cosubstrate coupled cofactor regeneration through the oxidation of 2 propanol to acetone,[29] we also tested these conditions. Indeed, similar stereo selectivities were observed for reduction of NDK **1** when 5% (v/v) 2 propanol was added as cosubstrate. However, the LbADH SBP productivity was found to be lower due to additional oxidation of 2 propanol to acetone (Figure S2). As expected,[28] the (*S*) selective Gre2p SBP revealed an extra ordinary high *anti* selectivity toward the 5 nitro 1 keto moiety of NDK **1**. This led to the exclusive formation of (*S*) anti hydroxyketones **2b**, which was slowly further reduced to pseudo C_2 diol **3a** (Figure S3B).

We then tested the specific enzyme loading of commercially available, STV functionalized superparamagnetic microbeads (MB STV, 2.7 μm diameter) that have a nominal binding capacity of ~200 pmol biotinylated peptide per mg MB. To this end, MB STV were incubated with an excess of the purified enzymes for 30 min and then isolated by magnetic separation.

The enzyme immobilization on the MBs (enzyme@MB) was verified by SDS PAGE (Figure S4), and the binding capacity was estimated by comparative grayscale analysis (Figure S5). Furthermore, specific activities of the immobilized enzymes were determined by chiral HPLC. The results are summarized in Table 1. The data in Table 1A indicate that similar amounts of all three enzymes were immobilized on MB STV with an average of about 240 pmol of subunits per mg MB. Given that it is difficult to predict the binding capacity of the SBP tagged enzymes because the SBP peptide simultaneously interacts with two of the four STV subunits,[30] these results are in very good aggreement with the expectation. Furthermore, determination of the catalytic activity of free and MB STV immobilized enzymes revealed that the immobilization did not substantially affect the activity and the stereoselectivity of the bead bound enzymes (Table 1B).

We then used the enzyme coated microbeads to setup a compartmentalized microfluidic packed bed reactor consisting of a poly(methyl methacrylate) (PMMA) chip that contains four microchannels (58.5 × 1.0 × 0.2 mm), each with a volume of about 11.7 μL (Figure 1).[31] Rectangular Nd magnets are located underneath the microchannels to retain up to 4.5 mg of the superparamagnetic enzyme@MB particles that are loaded by simple infusion of a bead suspension. Since the channels can be connected to each other in an arbitrary fashion, fluidic microreactors with up to four different compartments can be readily assembled (for specific examples, see Figures 2, 3 and Figure S6). The chips are integrated in a temperature controlled microfluidic mount that creates a standardized chip to world interface for connection with a fluidic system, where substrate solution is actively pumped through the microchannels into an automated fraction collector using a computer controlled syringe pump (Figure S6). Typically, reactions were conducted at 30 °C with a flow rate of 1 μL/min that results in a residence time of about 7 min per compartment. The outflow was fractionated automatically in 96 well plates, which contained NaClO to stop all enzymatic reactions. The samples were subsequently analyzed by chiral HPLC.

Initial investigations were carried out with a microfluidic chip that was equipped with only one enzyme for the reduction of NDK **1**. Owing to the capability of LbADH to harness 2 propanol oxidization for NADP(H) regeneration, we chose this system to investigate the long term stability and the robustness of the reactor against 2 propanol and acetone. Indeed, in the presence of 5% (v/v) organic solvents, we found that enzyme immobilization was highly stable thus allowing to operate the reactor for up to 350 h/14.5 days without any significant decrease in the enzyme's activity or stereoselectivity (Figure S7). This result impressively demonstrated the robustness of both the microfluidic device and the immobilized enzyme.

We then tested the fluidic reduction of NDK **1** using the two enzyme system composed of the (*R*) selective LbADH SBP@MB STV and GDH SBP@MB STV (Figure 2A). To this end, batches of enzyme loaded beads were prepared as described above and 0.5 mg LbADH SBP@MB STV and 4 mg of GDH SBP@MB STV beads were mixed and filled into the microchannel (blue channels, in Figure 2). The 1:8 ratio was chosen to account for the differences in the relative activity of the two enzyme functionalized microbeads (Table 1B). Similar, 1.5 mg of Gre2p SBP@MB STV and 3 mg of GDH SBP@MB STV were used to prepare compartments for the (*S*) selective reduction reactions (red channels, in Figure 2,

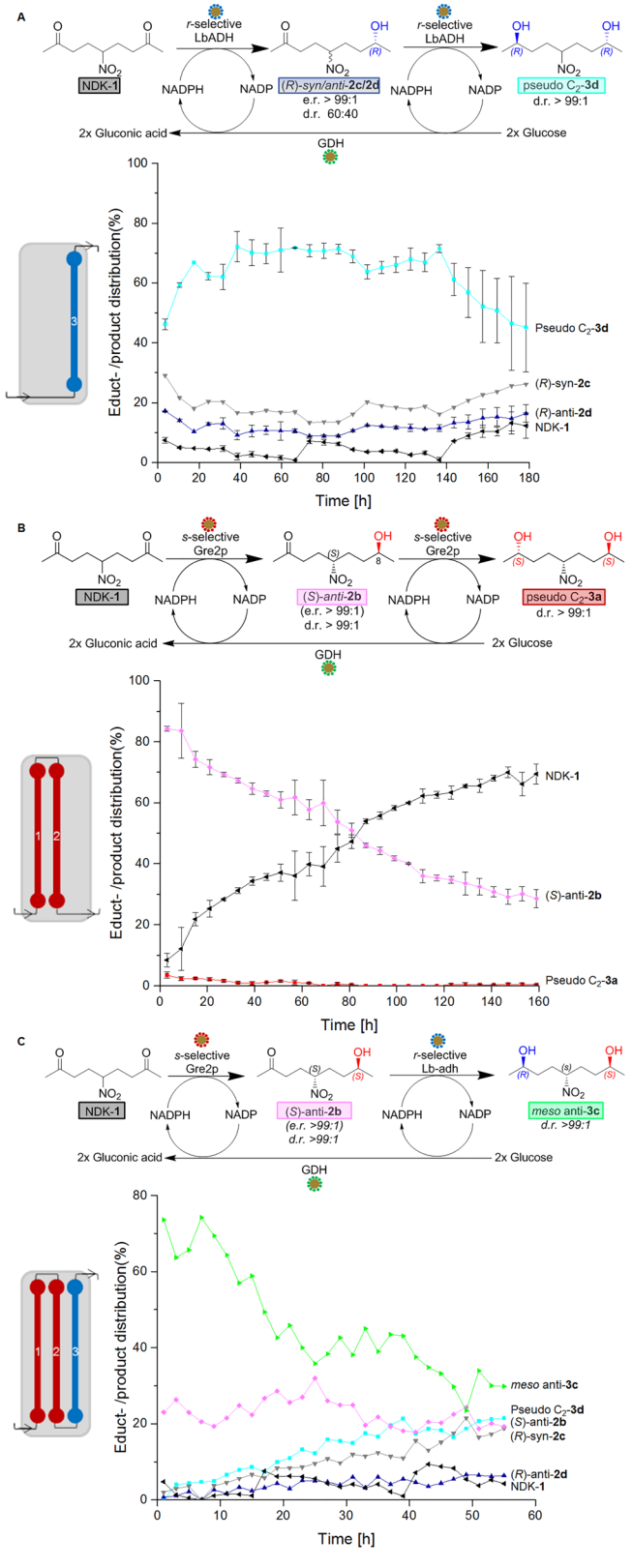

Figure 2. Stereoselective reductions of NDK **1** in compartmentalized microfluidic packed bed reactors. Each compartment contains either LbADH SBP@MB STV and GDH SBP@MB STV in an about 8:1 ratio (illustrated by the blue symbol) or Gre2p SBP@MB STV and GDH SBP@MB STV in an about 2:1 ratio (red). Chip configurations and reaction schemes are shown above the corresponding product formation graphs. The curves show the amounts of educt/products determined in the outflow of the reactor by chiral HPLC. Note that

Figure 2. continued

the blue module (A) exclusively generates (*R*) configured hydroxyketones **2c**/**d** and diol **3d** products, (B) whereas the red module produces only the (*S*) configured hydroxyketone **2b**. (C) In the coupled reaction where two red and one blue module are coupled sequentially, only a single product (*meso* anti diol **3c**) is formed in the initial phase of the reaction. For an image of the coupled reactor, see Figure S6.

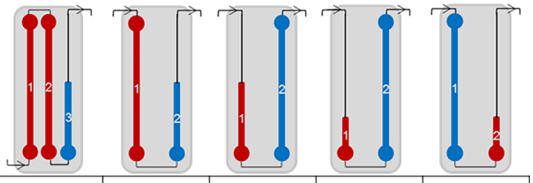

Setup	A	B	C	D	E
Ratio Gre2p:LbADH	4:1	2:1	1:2	1:4	1:4
3c/**3d** d.r. (3±1h)	95:5	75:25	60:40	45:55	2:98

Figure 3. Variation of the diastereomeric ratios (d.r. **3c**:**3d**) of diols **3** produced in differently configured microreactors containing variable relative amounts of bead immobilized enzymes (Gre2p SBP@MB STV, LbADH SBP@MB STV) with soluble GDH as NRE (see also Figure S9).

discussed below). As indicated in Figure 2A, the fluidic conversion of NDK **1** with only the (*R*) selective (blue) compartment led to the exclusive formation of (*R*) configured products. Again, the stable conversion rates over at least 5 days confirmed the good long term stability of the enzyme immobilization by the SBP tag.

Next, the (*S*) selective reduction of NDK **1** was performed by using two interconnected red compartments, each filled with Gre2p SBP@MB STV and GDH SBP@MB STV. Two compartments were used here to account for the lower activity of Gre2p as compared to LbADH (Table 1B) and to ensure high conversion rates when the two enzymes are fluidically coupled. We found that (*S*) anti hydroxyketone **2b** was produced over >6 days (Figure 2B). The conversion slightly decreased linearly from >84% to about 30% with a rate of about 8% per day. We assume that this decrease occurred due to a loss of enzyme activity over time (see also Figure S11).

We then investigate the two step reduction of NDK **1** by serial connection of two red (Gre2p) and one blue (LbADH) compartments to facilitate the initial (*S*) selective conversion of **1** to hydroxyketone **2b** and its subsequent (*R*) selective reduction to form the *meso* anti configured diol **3c**. It is shown in Figure 2C that the reactor selectively produced the desired product with an initial conversion of 73.6% (d.r. > 99:1). The slight decrease in the stereoselectivity (>94:6 after 3 ± 1 h) is assigned to the above discussed decrease of Gre2p SBP@MB STV activity (Figure 2B). Very importantly, this two step conversion of **1**, carried out with the same amount of enzymes in a one pot reaction, led to formation of mainly pseudo C_2 configured diol **3d** (58.6%) along with the *meso* anti diol **3c** (37.6%) with a significantly lower stereoselectivity (d.r. 39:61, Figure S8). These results clearly demonstrate the

Table 2. (A) Specific Enzyme Loading and (B) Activities of Free and Microbead Immobilized Enzymes

A	MW	Homomeric subunits	Specific enzyme loading[a]	
	[$g_{protein}$ $mol_{subunit}^{-1}$]		[$\mu g_{protein}$ mg_{MB}^{-1}]	[$pmol_{subunit}$ mg_{MB}^{-1}]
GDH-SBP-Crude@MB-STV	36598	4	5.5 ± 0.2	150 ± 5
LbADH-SBP-Crude@MB-STV	32338		6.4 + 0.2	198 ± 9
Gre2p-SBP-Crude@MB-STV	46640	1	7.0 ± 0.7	150 ± 15
Gre2p-HOB@MB-CH	72676		3.7 ± 0.7	51 ± 10
Gre2p-HOB-Crude@MB-CH			2.6 ± 0.1	36 ± 1

B	MW	Homomeric subunits	Specific activty[b]		
	[$g_{protein}$ $mol_{subunit}^{-1}$]		[$nmol_{substrate}$ min^{-1} mg_{MB}^{-1}]	[$\mu mol_{substrate}$ min^{-1} $mg_{protein}^{-1}$]	[$\mu mol_{substrate}$ min^{-1} $\mu mol_{subunit}^{-1}$]
GDH-SBP-Crude@MB-STV	36598	4	5.6 ± 0.8	1.0 ± 0.2	37 ± 7
GDH-SBP@MB-Epoxy			<1.0	-	-
LbADH-SBP-Crude@MB-STV	32338		66 ± 1.3	10.3 ± 0.7	333 ± 22
LbADH-SBP@MB-Epoxy			20.8 ± 0.1	-	-
Gre2p-SBP-Crude@MB-STV	46640	1	14.4 ± 0.3	2.1 ± 0.2	96 ± 12
Gre2p-SBP@MB-Epoxy			5.1 ± 0.3	-	-
Gre2p-HOB	72676		-	2.5 ± 0.03	182 ± 2
Gre2p-HOB@MB-CH			9.0 ± 2.2	2.4 ± 1.1	177 ± 77
Gre2p-HOB- Crude@MB-CH			5.5 ± 0.1	2.1 ± 0.1	154 ± 9
Gre2p-ST	40804		-	5 ± 0.1	204 ± 4
Gre2p-ST@MB-SC[c]			19.1 ± 0.2	-	-
Gre2p-ST-Crude@MB-SC[c]			20.6 ± 0.6	-	-

[a]Specific enzyme loading normalized to protein subunits analyzed by comparative grayscale analysis. Data represent the mean of triplicate analyzes ±1 SD. [b]Specific activities of immobilized and free LbADH, Gre2p, and GDH using NDK **1** and glucose as substrates. Data represent the mean of at least triplicate analyzes ± 1 SD, calculated as noted in Table 1. [c]Note that the quantitative comparison of immobilized and free Gre2p ST was hampered by the fact that the covalent ST/SC binding prevented stripping and thus quantification of the amount of bead bound protein.

utility of our compartmentalized reactor system for stereo selective multistep reactions.

To further analyze how the overall diastereoselectivity can be influenced by the microreactor configuration, we varied the enzyme ratios and flow direction. To enable a higher loading of each compartment with KRED@MB, we added soluble GDH into the continuous flow phase instead of employing the bead immobilized GDH SBP. Hence, each compartment could now hold up to 4 mg of KRED@MB. A series of experiments was conducted with differently configured microreactors, in which the relative amounts of the bead immobilized enzymes Gre2p SBP@MB STV and LbADH SBP@MB STV was varied from 4:1 to 1:4 (Figure 3). The reduction of NDK **1** was carried out under the usual conditions (30 °C, 1 μL/min flow rate), and the outflow of the reactor from 2 to 4 h was pooled (120 μL) and analyzed by chiral HPLC. The results clearly indicated that product ratios of *meso* anti diol **3c** and pseudo C_2 diol **3d** could be adjusted from a nearly exclusive formation of **3c** (d.r. 95:5, Figure 3A) to the nearly quantitative formation of **3d** (d.r. 98:2, Figure 3E). The product ratios obtained with reactor configurations A−D are in agreement with the expectations drawn from the data in Figure 2. Presumably due to the higher KRED@MB loading, the processes involving soluble GDH showed in setup A−C almost quantitative conversion of NDK **1** to diol **3** (>95%), which was higher than that obtained with coimmobilized GDH SBP (73.6%). Altogether, the results nicely illustrate the high modularity of this microreactor system which enables the convenient configuration to control the stereoselectivity of the two step biocatalytic transformation.

To further illustrate the scope of our concept of using self immobilizing fusion enzymes for biocatalytic flow processes, we then tested additional genetically encoded tagging systems for their suitability to immobilize functional enzymes. On the basis of our experience from cell surface display of orthogonal binding motifs,[34] we chose the SpyTag/SpyCatcher system, which is based on the SpyCatcher (SC, 113 aa) protein that forms a covalent isopeptide bond between one of its lysines and an aspartate residue of the 13 aa SpyTag (ST) peptide.[26] Furthermore, we used the self labeling Halo based oligonucleotide binder (HOB) tag protein (293 aa), that forms a covalent bond with small molecule chlorohexane (CH) ligands in a similar fashion as the regular Halo tag, commonly used for imaging in cell biology.[27] HOB was genetically engineered to bind to CH ligands attached to DNA oligonucleotides and DNA nanostructures with a significantly higher efficiency than Halo.[35]

Since protein purification is costly and time consuming and may even lead to a decrease in the enzymatic activity, we tested the direct immobilization of our orthogonally tagged enzymes from crude cell extracts. We chose Gre2p as model enzyme because it is less stable than GDH and LbADH (Table S4), and it is also barely amenable to nonspecific covalent immobilization on expoxy activated microbeads (Table 2B). The ST and HOB tags were genetically fused, together with an additional His tag, to the C terminus of Gre2p and the plasmids were overexpressed in *E. coli*. The three Gre2p variants were initially purified to homogeneity by Ni NTA chromatography (Figure S1) to determine their specific activity (Table 2). The appendence of different tags affected the specific activity of the free enzymes slightly. Gre2p HOB and Gre2p ST were almost twice as active as the Gre2p SBP (Table 2B).

The purified enzymes were then allowed to bind to magnetic microbeads coated with the cognate binding partner. For this purpose, MB STV was used as described above for the capture of Gre2p SBP. Else, the beads were modified with a Biotin PEG chlorohexyl linker to generate MB CH for capture of Gre2p HOB. Furthermore, commercially available amino reactive magnetic beads (Dynabeads M 270 Epoxy) were coated with recombinant SC protein to generate MB SC for the capture of Gre2p ST. After capture and magnetic separation, all three Gre2p coated MB formulations showed enzymatic activity and generated exclusively (*S*) anti hydroxyketone **2b**, as expected (Table 2).

Similar binding experiments, carried out with crude cell extracts instead of the purified enzymes, clearly showed that the resulting quality of the beads was comparable to that obtained from the purified enzymes (Tables 1B, 2B, Figure S10). A moderate reduction (<40%) of the binding capacity was notable in some cases (compare Tables 1A, 2A), presumably due to blocked binding sides because of unspecific protein adsorption. Notably, we also tested the competitive binding of LbADH SBP, Gre2p HOB and Gre2p ST crude extracts to MB STV. The isolated beads revealed the specific formation (*R*) configured hydroxyketones **2c**/**d** and diol **3d** products (Table S5), thereby indicating that exclusively the LbADH SBP@MB STV had been formed. A direct comparison of compartmentalized bioreactors equipped with beads bearing either SBP , HOB , or ST modified enzymes (Gre2p SBP@MB SBP, Gre2p HOB@MB CH, or Gre2p ST@MB SC, respectively, in Figure S11) revealed that the three tags are well suited for immobilization in a flow reactor. This finding is important because orthogonal tags could be used in future applications for the direct and site specific immobilization of enzymes on beads under flow conditions. Therefore, these results suggest that the employment of self immobilizing fusion enzymes may open the door to dispense the need for laborious biocatalyst purification and also ease the production of compartmentalized reactors.

In conclusion, we herein demonstrated the use of self immobilizing fusion enzymes for the specific and highly modular configuration of compartmentalized flow reactors. In principle, such biocatalysts can be used without extensive purification, thereby significantly reducing time and costs of production processes with a concomitant increase in flexibility for research applications. We here used KREDs for stereo selective multistep syntheses as a proof of concept. However, our approach should also be applicable for many other enzymes. Hence, we believe that compartmentalized microfluidic packed bed reactors equipped with self immobilizing fusion enzymes will be useful for a variety of other biocatalytic or chemo enzymatic cascade reactions.

■ ASSOCIATED CONTENT

● Supporting Information

The Supporting Information is available free of charge on the ACS Publications website at DOI: 10.1021/acscatal.7b02230.

Experimental procedures and materials, further product analysis, enzyme characterization, additional reactor, and bead experiments, including Figures S1−S11 and Tables S1−S5 (PDF)

■ AUTHOR INFORMATION

Corresponding Author

*E mail: niemeyer@kit.edu. Tel./Fax: + 49 (0)721 608 2 5546.

ORCID

Theo Peschke: 0000 0002 6775 1410

Christof M. Niemeyer: 0000 0002 8837 081X

Author Contributions

All authors have given approval to the final version of the manuscript.

Notes

The authors declare no competing financial interest.

■ ACKNOWLEDGMENTS

This work was supported by the Helmholtz program BioInterfaces in Technology and Medicine and Deutsche Forschungsgemeinschaft (Ni399/15 1). We thank Anke Dech, Maximilian Grösche and CorneliaZiegler for experimental help.

■ REFERENCES

(1) Straathof, A. J. *Chem. Rev.* **2014**, *114*, 1871−1908.
(2) Bornscheuer, U. T.; Huisman, G. W.; Kazlauskas, R. J.; Lutz, S.; Moore, J. C.; Robins, K. *Nature* **2012**, *485*, 185−194.
(3) France, S. P.; Hepworth, L. J.; Turner, N. J.; Flitsch, S. L. *ACS Catal.* **2017**, *7*, 710−724.
(4) Quin, M. B.; Wallin, K. K.; Zhang, G.; Schmidt Dannert, C. *Org. Biomol. Chem.* **2017**, *15*, 4260−4271.
(5) Wheeldon, I.; Minteer, S. D.; Banta, S.; Barton, S. C.; Atanassov, P.; Sigman, M. *Nat. Chem.* **2016**, *8*, 299−309.
(6) Kuchler, A.; Yoshimoto, M.; Luginbuhl, S.; Mavelli, F.; Walde, P. *Nat. Nanotechnol.* **2016**, *11*, 409−420.
(7) Chen, Z.; Zeng, A. P. *Curr. Opin. Biotechnol.* **2016**, *42*, 198−205.
(8) Mason, B. P.; Price, K. E.; Steinbacher, J. L.; Bogdan, A. R.; McQuade, D. T. *Chem. Rev.* **2007**, *107*, 2300−2318.
(9) Wohlgemuth, R.; Plazl, I.; Znidarsic Plazl, P.; Gernaey, K. V.; Woodley, J. M. *Trends Biotechnol.* **2015**, *33*, 302−314.
(10) Kim, D.; Herr, A. E. *Biomicrofluidics* **2013**, *7*, 041501.
(11) Fornera, S.; Kuhn, P.; Lombardi, D.; Schlüter, A. D.; Dittrich, P. S.; Walde, P. *ChemPlusChem* **2012**, *77*, 98−101.
(12) Boehm, C. R.; Freemont, P. S.; Ces, O. *Lab Chip* **2013**, *13*, 3426−3432.
(13) Schroeder, H.; Hoffmann, L.; Müller, J.; Alhorn, P.; Fleger, M.; Neyer, A.; Niemeyer, C. M. *Small* **2009**, *5*, 1547−1552.
(14) Bolivar, J. M.; Wiesbauer, J.; Nidetzky, B. *Trends Biotechnol.* **2011**, *29*, 333−342.
(15) Halim, A. A.; Szita, N.; Baganz, F. *J. Biotechnol.* **2013**, *168*, 567−575.
(16) Yamaguchi, H.; Honda, T.; Miyazaki, M. *J. Flow Chem.* **2016**, *6*, 13−17.
(17) Britton, J.; Dyer, R. P.; Majumdar, S.; Raston, C. L.; Weiss, G. A. *Angew. Chem., Int. Ed.* **2017**, *56*, 2296−2301.
(18) Mukai, C.; Gao, L.; Bergkvist, M.; Nelson, J. L.; Hinchman, M. M.; Travis, A. J. *PLoS One* **2013**, *8*, e61434.
(19) Mukai, C.; Gao, L.; Nelson, J. L.; Lata, J. P.; Cohen, R.; Wu, L.; Hinchman, M. M.; Bergkvist, M.; Sherwood, R. W.; Zhang, S.; Travis, A. J. *Angew. Chem., Int. Ed.* **2017**, *56*, 235−238.
(20) Dorn, I. T.; Neumaier, K. R.; Tampe, R. *J. Am. Chem. Soc.* **1998**, *120*, 2753−2763.
(21) Bolanos Garcia, V. M.; Davies, O. R. *Biochim. Biophys. Acta, Gen. Subj.* **2006**, *1760*, 1304−1313.
(22) Terpe, K. *Appl. Microbiol. Biotechnol.* **2003**, *60*, 523−533.
(23) Rabe, K. S.; Müller, J.; Skoupi, M.; Niemeyer, C. M. *Angew. Chem., Int. Ed.* **2017**, *56*, 13574−13589.
(24) Keefe, A. D.; Wilson, D. S.; Seelig, B.; Szostak, J. W. *Protein Expression Purif.* **2001**, *23*, 440−446.
(25) Zhao, X.; Li, G.; Liang, S. *J. Anal. Methods Chem.* **2013**, *2013*, 581093.
(26) Zakeri, B.; Fierer, J. O.; Celik, E.; Chittock, E. C.; Schwarz Linek, U.; Moy, V. T.; Howarth, M. *Proc. Natl. Acad. Sci. U. S. A.* **2012**, *109*, E690−7.
(27) Los, G. V.; Wood, K. *Methods Mol. Biol.* **2007**, *356*, 195−208.
(28) Skoupi, M.; Vaxelaire, C.; Strohmann, C.; Christmann, M.; Niemeyer, C. M. *Chem. Eur. J.* **2015**, *21*, 8701−8705.
(29) Leuchs, S.; Greiner, L. *Chem. Biochem. Engin. Q.* **2011**, *25*, 267−281.
(30) Barrette Ng, I. H.; Wu, S. C.; Tjia, W. M.; Wong, S. L.; Ng, K. K. *Acta Crystallogr., Sect. D: Biol. Crystallogr.* **2013**, *69*, 879−887.
(31) Kampe, T.; Konig, A.; Schroeder, H.; Hengstler, J. G.; Niemeyer, C. M. *Anal. Chem.* **2014**, *86*, 3068−3074.
(32) Breicha, K.; Muller, M.; Hummel, W.; Niefind, K. *Acta Crystallogr., Sect. F: Struct. Biol. Cryst. Commun.* **2010**, *66*, 838−841.
(33) Hilt, W.; Pfleiderer, G.; Fortnagel, P. *Biochim. Biophys. Acta, Protein Struct. Mol. Enzymol.* **1991**, *1076*, 298−304.
(34) Peschke, T.; Rabe, K. S.; Niemeyer, C. M. *Angew. Chem., Int. Ed.* **2017**, *56*, 2183−2186.
(35) Kossmann, K. J.; Ziegler, C.; Angelin, A.; Meyer, R.; Skoupi, M.; Rabe, K. S.; Niemeyer, C. M. *ChemBioChem* **2016**, *17*, 1102−1106.